# 12 Energy Management Strategy for Electric Vehicles and Connected Renewable Energy Systems in a Micro Grid Environment of a University Campus

Bedatri Moulik, Bibaswan Bose, Ahmed M. Ali und Dirk Söffker

## Inhaltsverzeichnis



B. Moulik (✉)
Department of Electrical and Electronics Engineering, Amity School of Engineering and Technology, Amity University, Noida, India
E-Mail: bmoulik@amity.edu

B. Bose
EVI Technologies Pvt. Limited, New Delhi, India

A. M. Ali
The Egyptian Ministry of Defense, Cairo, Egypt
E-Mail: ahmed.ali@uni-due.de

D. Söffker
Chair of Dynamics and Control, University of Duisburg-Essen, Duisburg, Germany
E-Mail: soeffker@uni-due.de



H. Proff (Hrsg.), *Transforming Mobility – What Next?*,
https://doi.org/10.1007/978-3-658-36430-4_12

## 12.1 Introduction

The future of electric vehicles (EVs) in reducing carbon footprints depends on the introduction of more and more EVs in smaller communities like university campuses. In combination, integrated systems must be developed with a maximum of renewable energy utilization to charge the EVs. In a microgrid environment with EVs and home load demand connected together with multiple renewables, the need for energy management system is vital. In the presence of multiple energy sources, optimally guiding the power flow between the components is a task of energy management (M. Ali et al., 2020). Several goals can be identified within an EMS, such as maximization of energy utilization, guaranteeing user satisfaction, minimization of daily electricity cost, or maximization of battery life. However, most of these objectives are interrelated, each playing a significant role in the performance of EMS.

Electric vehicle- connected integrated systems are considered in literature, using solar and energy storage systems based charging in (Patterson et al., 2015) whereas grid-tied solar-battery storage systems in (Gautham Ram Chandra Mouli et al., 2019; Chaudhari et al., 2018; Patterson et al., 2015) Fuel cells as energy conversion systems are considered in (Gautham Ram Chandra Mouli et al., 2019; Patterson et al., 2015; Robledo et al., 2018) Wind, solar, and battery storages are considered in (Marzband et al., 2013). Considering the existence of various sources/storages and loads in an integrated system, an optimal scheduling of charging services for EVs is essential (Eldeeb et al., 2018). The influence of the global architecture is discussed in (Cao et al., 2019; Ru et al., 2013), where in (Ru et al., 2013), an optimal sizing of the battery storage was considered. In (Eldeeb et al., 2017), sizing of solar battery storage is discussed for a university park with charging stations for EVs. Both the effect of PV size and number of connected EVs are analysed in (Zhong et al., 2018), whereas, technical and empirical aspects are considered in (G.R. Chandra Mouli et al., 2016). The seasonal, diurnal variations of PV power along with dynamic EV charging profiles are considered in (Koohi-Kamali et al., 2014). In (Cao et al., 2019), an optimal battery size for grid-connected PVs is discussed with reference to two objectives.

In (Marzband et al., 2013), an operational architecture for microgrid is considered with central control unit which implements an EMS based on local energy market. Based on day-ahead scheduling, power set points of energy sources are calculated. Furthermore the best purchasing price from the customer's point of view is presented. In (Stluka et al., 2011), different aspects of microgrid EMS are highlighted. Optimization with respect to supply side, demand side, and storage performance, respecting various constraints and maintaining user expectations has to be applied to solve the complex mathematical problem. In (Bhatti et al., 2016),

a multi-objective optimization (MOO) is considered for minimization of electricity cost and maximization of battery life, satisfying certain constraints. A similar set of objectives is considered in (Robledo et al., 2018). The stochastic nature of the types of EVs and their varied arrival times was considered. The pareto front of solutions obtained from the contradicting objectives was subjected to a Utopia operation point that obtains the best results with each objective considered separately. However, further possibilities should include user preferences and user driving patterns to design the EMS from a driver's perspective than grid-perspective. The optimization should also focus on energy efficiency by maximizing the use of renewables. Energy management can be formulated (Mokrani et al., 2014) as an offline causal problem assuming known operational parameters of power sources, storage components, loads, and user demands; or online as non causal optimization problem (Robalino et al., 2009; Shi et al., 2017) which considers the stochastic nature of power generation and load demands. To solve such tasks, Lyapunov optimization is used in (Mokrani et al., 2014), game theory based approach in (Eldeeb et al., 2018), mixed integer linear programming in (Patterson et al., 2015), hybrid optimization for a shifting framework is proposed in (Milis & Peremans, 2015) for a EMS which switches between deterministic and rule-based approaches, stochastic semi-Markov decision process is used in (Robalino et al., 2009), and stochastic dynamic programming is used in (Wu et al., 2016). In (Wu et al., 2016), the randomness in the EV trip times and EV battery energy at plug-in time are modelled using Markov chains. In this contribution, an integrated microgrid environment is considered with renewables: solar PV, wind, battery energy storage connected to the grid via a DC bus. The loads include home load demand and charging of EV batteries, also connected to the DC bus. Four local controllers are considered for solar PV, wind energy system, bus voltage control, and EV charge control. A supervisory controller is also considered for balancing the power supply and demand, and maximizing the use of renewables wherever possible. Finally a charge scheduling is proposed for minimization of the user's electricity costs while maintaining the user satisfaction. Simulation results indicate the improvement in energy cost savings due to optimized charge scheduling of the EVs in an example scenario.

## 12.2 System Description

The complete system is shown in Fig. 12.1. The system consists of Solar Photo-Voltaic Array (SPVA), wind generator, Battery Energy Storage System (BESS), electric vehicle load, and residential load. All the systems are connected to an DC busbar of 22 kV. The Energy management System (EMS) performs the task of

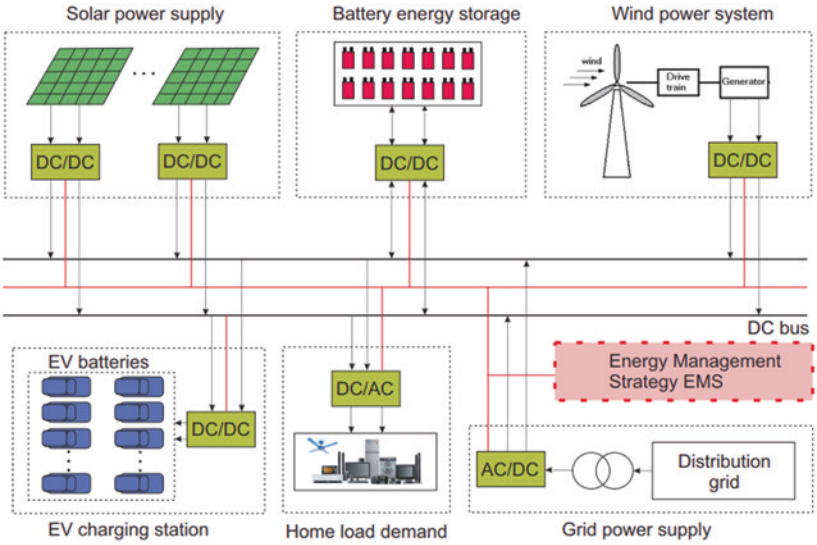


**Fig. 12.1** Complete system model of the microgrid

**Table 12.1** Component ratings and specifications

| Component | Specification |
|---|---|
| Solar PV array | 20 kV, 8 MW |
| Wind turbine generator | 450 V, 4.5 MW |
| Storage battery | 20 kV, 15 MW, 10 KAh |
| Home load | 10 MW, 0.15 power factor, 0.16 MVA |
| Electric vehicle load | 375 V, 10 KW, 106 Ah |

energy distribution and helps to increase the system efficiency by reducing the involvement of grid in the system. Further specifications are given in Table 12.1.

### 12.2.1 Battery

Two types of batteries are used. First, a battery energy storage system (BESS) to store the excess energy of PV generation which can be used later and second the electric vehicle battery. The mathematical modeling for both batteries is based

on 1RC model (Zhang et al., 2017) as described in Eq. (12.1). The mathematical equations are obtained by performing Laplace Transform on a 1RC model of a cell as,

$$V_T = V_{OCV} - \left( R_0 + \frac{\frac{R_1}{s}}{R_1 C_1 + \frac{1}{s}} \right) I, \tag{12.1}$$

where $R_0$, $R_1$ is the internal resistance of the cell and $C_1$ is the internal capacitance of the cell. Here, $V_{OCV}$ is the open circuit voltage and $V_T$ is terminal voltage. The SOC is computed as,

$$S0C = SOC(t_0) + \frac{1}{C_{rat}} \int_{t_0}^{t_0+\tau} I_{bat} dt. \tag{12.2}$$

### 12.2.2 Wind Energy Generator

Wind energy generator system consists of wind turbine blades that are connected to DC generator through a shaft that transfers energy to the generator. The equations are given by the mathematical expressions (12.3)–(12.6), to model the generator system. The wind turbine controller trips the wind generator and removes it from grid when speed of the wind exceeds a certain maximum value. The turbine returns to grid when wind has nominal value as,

$$V_t = E_a - I_a R_a, \tag{12.3}$$

$$I_a = I_F + I_L, \tag{12.4}$$

$$I_F = \frac{V_t}{R_{sh}}, \tag{12.5}$$

$$V_t = E_a - \left( \frac{V_t}{R_{sh}} + I_L \right) R_a, \tag{12.6}$$

where, $V_t$ represents the terminal voltage, $E_a$ the armature voltage, $I_a$ the armature current, $I_F$ the field current, $R_a$ the armature resistance and $R_{sh}$ the shunt resistance. The load current is represented by $I_L$.

### 12.2.3 Solar PV

The function of a solar photo voltaic array (SPVA) is to convert incident solar energy into electrical energy. The PV solar cell generates electricity when the

diode junction is excited by a solar radiation. The generation of electricity from PV solar cells is dependent on temperature and irradiation. Several PN junction diodes are connected together to form a cell and the interconnection of these cells form an array. PV cell output voltage ($V_C$) can be represented in Eqs. (12.7)–(12.14) (Alsumiri, 2019)

$$V_C = \frac{AkT_C}{e} \ln\left(\frac{I_{ph} + I_0 - I_C}{I_0}\right) - R_s I_C, \tag{12.7}$$

$$C_{TV} = 1 + B_T(T_A - T_X), \tag{12.8}$$

$$C_{TI} = 1 + \frac{Y_T}{S_C}(T_X - T_A), \tag{12.9}$$

$$C_{SV} = 1 + B_T a_S(S_X - S_C), \tag{12.10}$$

$$C_{SI} = 1 + \frac{1}{S_C}(S_X - S_C), \tag{12.11}$$

$$\Delta T_C = a_S(S_X - S_C), \tag{12.12}$$

$$V_{CX} = C_{TV} C_{SV} V_C, \tag{12.13}$$

$$I_{phX} = C_{TI} C_{SI} I_{ph}, \tag{12.14}$$

where, the variables are defined in Table 12.2.

### 12.2.4 DC/AC Converter

A two-step converter and a push–pull flyback converter has been used to regulate the voltage level followed by a full bridge inverter which converts DC into 3 phase AC signal. This is represented by the following equations,

$$O(t) = A * sin\big(\lfloor f * t \rfloor + \theta\big), \tag{12.15}$$

where, $O(t)$ is the output sine wave in terms of time, $A$ is the amplitude, $f$ is the frequency, $t$ is time and $\theta$ is the phase. Here the three phases have been differentiated by 120 degrees.

**Table 12.2** Solar PV symbols and their definitions

| Abbreviation | Detail |
|---|---|
| k | Boltzmann constant |
| $I_c$ | Cell output current |
| $S_c$ | Solar irradiation level |
| $T_a$ | Ambient temperature |
| $I_{phx}$ | Photocurrent output |
| $C_{TV}$ | Temperature voltage coefficient |
| $C_{TI}$ | Temperature photocurrent co-efficient |
| $C_{SV}$ | Solar irradiation voltage co-efficient |
| $\Delta T_C$ | Temperature change |
| $V_{CX}$ | Cell output Voltage |
| $I_0$ | Reverse saturation current of diode |
| $R_s$ | Series resistance of cell |
| $T_c$ | Reference cell operating temperature |
| $I_{ph}$ | Photocurrent's function of irradiation level and junction temperature |

### 12.2.5 DC/DC Converter

In this work, a boost converter used with solar and wind systems is based on the equations,

$$C\frac{dV_C}{dt} = (1-u)i_L - \frac{V_C}{R} - i_0, \tag{12.16}$$

$$L\frac{di_L}{dt} = V_{in} - (1-u)V_C, \tag{12.17}$$

where $V_c$ represents the capacitor voltage, $I_L$, the inductor current, $R$ the resistance, $L$ the inductance, $C$ the capacitance,$I_0$ the load current, $V_{in}$ the voltage input. CuK converter, a dual of buck boost DC-DC converter is used with the battery storage system. One of the main assets of using the CuK converter is that it has continuous input and output currents. The main equations are given as,

$$\dot{X}' = \begin{bmatrix} (-R_1/L_1) & 0 & (-1/L_1) & 0 \\ 0 & (-R_2/L_2) & 0 & (-1/L_2) \\ (1/C_1) & 0 & 0 & 0 \\ 0 & (1/C_2) & 0 & 0 \end{bmatrix} X + \begin{bmatrix} 0 & 0 & (D/L_1) & 0 \\ 0 & 0 & (-1/L_2) & 0 \\ (-D/C_1) & (D/C_1) & 0 & 0 \\ 0 & 0 & 0 & 0 \end{bmatrix} X + \begin{bmatrix} 1/L_1 & 0 \\ 0 & 0 \\ 0 & 0 \\ 0 & -1/C_2 \end{bmatrix} u. \tag{12.18}$$

Here, duty cycle is represented as D. The first A matrix represents the linear part and second A matrix represents the non-linear part.

## 12.3 Optimal Charge Scheduling and Energy Management

As summarized in (Mukherjee & Gupta, 2015), scheduling in a smart grid refers to the relation of timings of charging/discharging the EVs in a connected system. The aggregator is responsible for managing the individual charging actions of the EVs, acting as a link between generating and charging stations. The EVs are connected or rather grouped by aggregators controlling the scheduling, which can be either in a unidirectional (G2V) or bidirectional (V2G-G2V) scenarios. It can either be centrally controlled by the aggregator or decentralized where each EV takes the decision in co-ordination with the aggregator. Mobility-aware control can be achieved when arrival/departure, trip history, are also taken into account. In a mobility-aware, unidirectional, centralized control concept, determining the appropriate charging times of the connected EVs can be formulated as an optimization problem. Within the optimized charge scheduling framework, delivering reliable power to the customers, particularly in the presence of renewable energy sources is another task of the real time control strategy. Thus, in this contribution, an energy management problem focussing on the operational requirements and meeting the supply–demand balance is also considered.

### 12.3.1 Supervisory and Local Controllers

The main task of the supervisory controller is to check the power demand, power available from renewable energy sources, and calculate the power difference $P_{diff}$ , using,

$$P_{renewable} = P_{solar} + P_{wind}, \tag{12.19}$$

$$P_{diff} = P_{demand} - P_{renewable}. \tag{12.20}$$

If $P_{diff}$ is positive, it directs the usage of battery till the demand exceeds the energy available from the renewables. In that case, it directs the usage of the grid. For $P_{diff}$ equal to zero, no action is taken. For $P_{diff}$ negative, battery is charged from the grid. The modes of the supervisory control strategy is shown in Fig. 12.2.

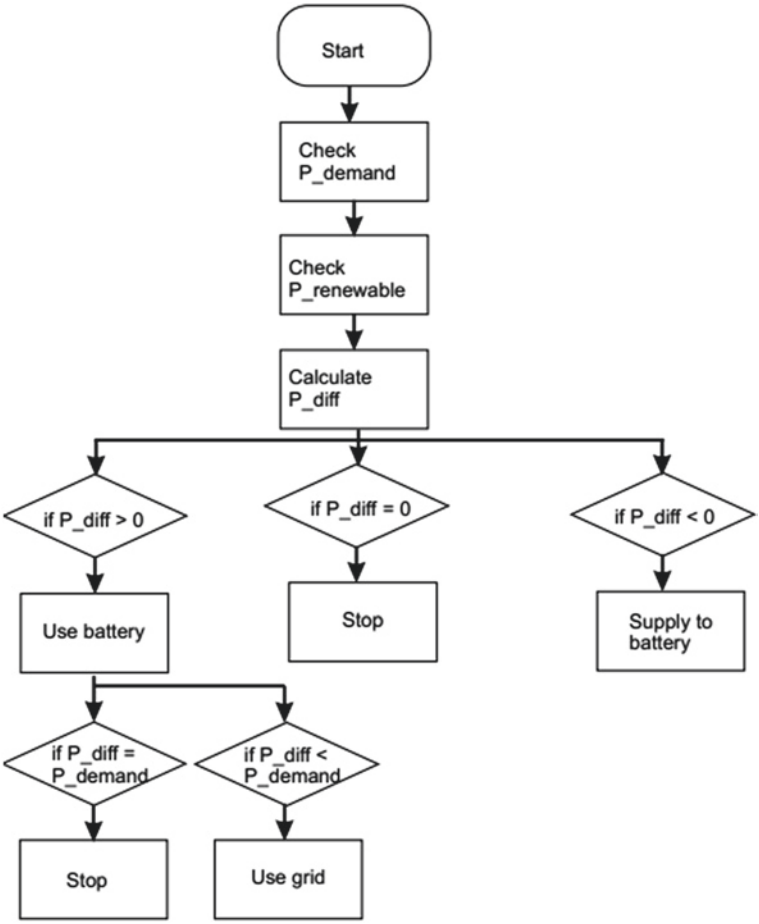


**Fig. 12.2** Supervisory control loop

As published in (Bose et al., 2020) the local controllers are responsible for DC bus voltage control, MPPT control of the solar PV, wind generator speed control, and EV charge control. As shown in Fig. 12.3, the MPPT algorithm for wind turbine with tip speed ratio technique, regulates the rotational speed of the generator. An optimal tip speed ratio is maintained at which power extracted is maximum (M. et al., 2013), as

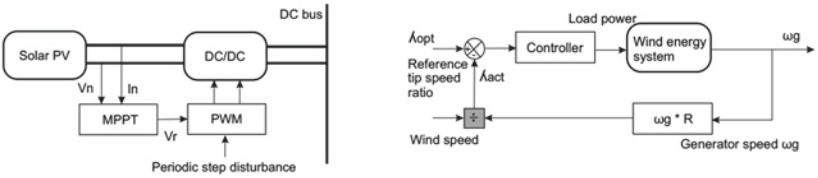


**Fig. 12.3** Control strategy used for wind and solar

$$P_{max} = K_{opt} + \omega_{opt}^3, \tag{12.21}$$

where,

$$K_{opt} = 0.5 * \rho A * (r_m/\lambda\, opt)^3 * C_{pmax}, \tag{12.22}$$

$$\omega_{opt} = \lambda opt/r_m * u. \tag{12.23}$$

The MPPT algorithm is also used to allow the solar PV to operate at its maximum power output point. This is explained in Fig. 12.3. As mentioned in (Liu et al., 2019) a disturbance observation method is used where a periodic constant step disturbance is applied to the output voltage of the PV array as ΔV,

$$\frac{dP}{dV} = \frac{d(IV)}{dV} = I + V\frac{dI}{dV}, \tag{12.24}$$

$$\frac{\Delta P}{\Delta \mathrm{V}} \begin{cases} > 0 & (\textit{current source region}) \\ = 0 & (\textit{maximum power point}) \\ > 0 & (\textit{voltage source region}) \end{cases}.$$

A DC bus voltage control method is used as shown in Fig. 12.4. The bi-directional DC/DC converter connected to the battery energy storage system is subjected to switching signals, generated by controlling the duty cycle D as,

$$\frac{V_{in}}{V_{out}} = -\frac{D}{1-D}, \tag{12.25}$$

which is varied using a PI controller as,

$$D = \frac{k_1 + k_2 s}{s}(V_{ref} - V_{out}), \tag{12.26}$$

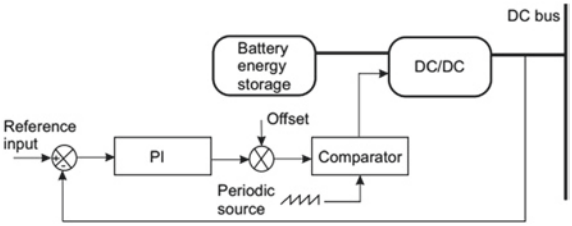


**Fig. 12.4** Control strategy for DC bus voltage regulation

here, $k_1$ and $k_2$ are constants. A list of variables is given in Table 12.3.

A charge control scheme is applied for controlling the charging of EV batteries as shown in Fig. 12.5. The first loop of control is for overcharge protection and here, the SOC of each EV battery is checked if exceeding 90 %. The second stage is for finding whether the SOC is within an optimal boundary. The optimal boundaries can be determined via an offline optimization process. The main idea is to define an objective function based on user electricity consumption and preferences, and schedule the charging of EVs accordingly to achieve the best of both objectives. In other words, the user's electricity costs are minimized by scheduling the charging of EVs during off peak hours while

**Table 12.3** Controller symbols and their definitions

| Abbreviation | Details |
|---|---|
| $C_p$ | Turbine power co-efficient |
| $\rho$ | Air density |
| A | Turbine sweeping area |
| u | Wind speed |
| $\lambda$ | Tip speed ratio |
| $r_m$ | Turbine rotor radius |
| $\omega$ | Angular velocity of turbine |
| $V_n$, $I_n$ | Bus voltage and current |
| $V_b$, $I_b$ | Reference voltage and current |
| $V_r$ | Periodic disturbance |
| D | Reverse saturation current of diode |
| $V_{ref}$ | Reference bus voltage |
| $V_{out}$ | Output voltage |

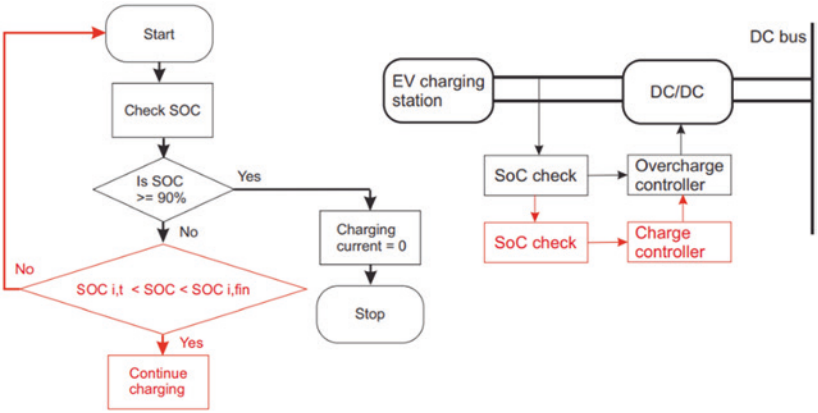


**Fig. 12.5** Control logic for overcharge protection and charging control of the EV batteries

considering the arrival times and deadlines specified by each EV user. This is to ensure that charging is optimally distributed but at the same time charging is completed before the deadline.

### 12.3.2 Optimization

An optimization problem is formulated (Chung et al., 2018) for minimizing the user's charging cost $J_1$ and maximizing the user's convenience $J_2$ as given in Eqs. (12.27) and (12.29). The first objective function is given as

$$J_1 = \sum_{t=1}^{T} C_t \tag{12.27}$$

where, $C_t$, the cost of EV charging at time t is given as,

$$C_t = \int_{L_1^{base}}^{z_t} g(z)dz = k_0\left(z_t - L_1^{base}\right) + \frac{k_1}{2}\left(z_t^2 - L_1^{base^2}\right), \tag{12.28}$$

here, $L_1^{base}$ represents the base load and $z_t$ the total load in time slot $t$. The constants here are $k_0$ and $k_1$.

The second objective function is given as

$$J_2 = \sum_{t=1}^{T} \sum_{i=1}^{N} u_{i,t} \tag{12.29}$$

Where, EVs are numbered from $i$ to $N$ and $u_{i,t}$ represents the user convinience as,

$$u_{i,t} = \frac{1}{w^*_{i,t}, w_{i,t}} \tag{12.30}$$

Here, $w^*_{i,t}$ represents the minimum number of time slots needed to charge ith EV;$t$ represents the starting of time slot. Thus the charging task of ith EV can not be completed before $t + w^*_{i,t}$.

$$w^*_{i,t} = \frac{(SOC_i^{fin} - SOC_{i,t})E_i^{cap}}{P_{i,max}} \tag{12.31}$$

The battery's capacity is represented as $E_i^{cap}$, SOC of ith EV as $SOC_i$, and maximum charging rate of EV limited by power $P_{i,max}$. The other parameter, $w_{i,t}$ represents the number of time slots remaining till ith EV is charged before its deadline $r_i$. It is given as,

$$w_{i,t} = r_i - t \tag{12.32}$$

The total objective function can be represented as.

$$J(x) = \min\{J_1, -J_2\}; \quad \text{where} \quad x = [z_t, SOC_i, SOC_i^{fin}] \tag{12.33}$$

Considering an architecture with a central aggregator (CA) connected to multiple charging stations can be considered as shown in Fig. 12.6. An optimal charge scheduling can be considered to be implemented at the CA. The CA is connected to $M$ charging stations with $M$ EVs. An $EV_i$ can have $SOC_{i,t}$ at time slot $t$. The target maybe to get charged upto $SOC_i^{fin}$. Let $a_i$ be the arrival time of the ith EV and $r_i$ be its deadline. An assumption here [8] is that an EV can finish charging before $r_i$ but not after $r_i$. If $H = \{1, 2, \ldots M\}$ be the set of EVs connected in $M$ charging stations and $W = \{1, 2, \ldots K\}$ be the sliding time window of all time slots spanned; then a case with four EVs is shown in Fig. 12.6. Here, at the current time slot t = 3, $H = \{2, 3, 4\}$ as during this current time slot onwards, EVs 2, 3, and 4 are charging; $W = \{3, 4, 5, 6, 7\}$ as the sliding time window covers all time slots starting from current time window until when the last EVs is charging, the last EV 4 completes charging at time slot 7. The charge scheduling problem is then defined for the entire time horizon T with equal time slots $t = \{1, 2, \ldots t\}$. The optimization is solved using Multi-objective Genetic Algorithm (MOGA).

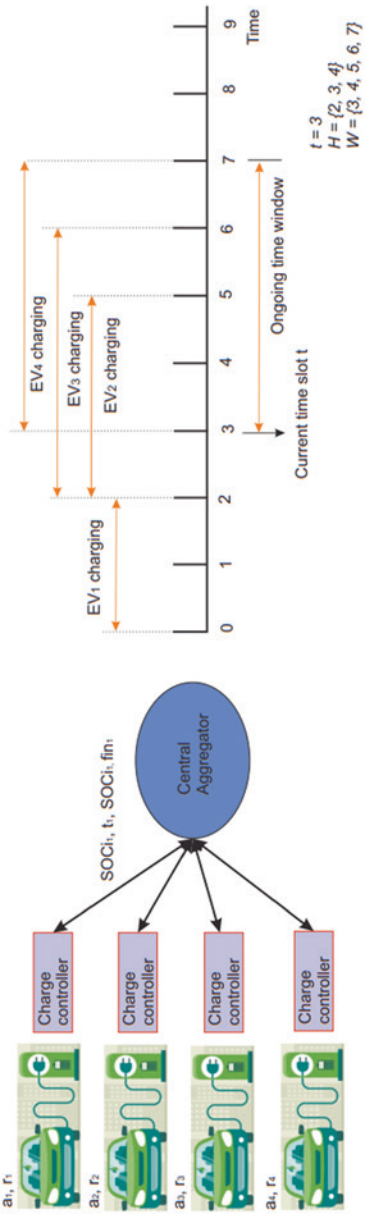


**Fig. 12.6** An example of optimal charge scheduling

## 12.4 Simulation and Results

For the designed prototype with a grid capacity 10 MW and grid electricity prices for India considered to be 16 ₹/kWh, it can be assumed that 100, Hyundai Kona EVs can be charged at charging rate 21 kWh using a DC fast charger. In a worst-case scenario where all EVs are being charged together along with home load demand being 7 MW on an average day is shown in Fig. 12.7. In Fig. 12.7, the forecasted wind and solar powers on an average day is shown and the grid consumption in the worst-case scenario is simulated. The average electricity prices borne by the EVs and home load at different times of the day is shown in Fig. 12.8. As shown in Fig. 12.9, as per the considered energy management strategy, the power demanded will still be fulfilled by the power supplied. Higher demand will also lead to sharp decline in BESS SOC as shown in Fig. 12.10. Next a case scenario is designed for ten EVs which is better than the worst-case scenario with the EVs not being charged at the same time but charging is randomly distributed over a period of time. A total of 10 EVs are considered to be charging at different intervals as shown in Fig. 12.11. The initial SOCs are assumed to have values given in Table 12.4. The arrival times and deadlines of each EV are also defined. The final SOCs are different for each EV indicating different charging schedules. In this contribution, only final SOC and charging time slot, are considered as optimization variables, however, initial SOC can also be considered if the driving profiles of individual drivers are realized.

Finally, the optimized case scenario is designed with EVs distributed as given in Table 12.5. The corresponding optimized charging costs are also indicated in Table 12.5. Here, considering the same initial SOCs, for the same ten EVs, with the same arrivals and deadlines given in Table 12.4; the final values of SOC are optimized. A benefit is achieved in terms of charging cost due to optimal charging distribution. For example, EV7 which arrives at 11:30 and will leave at 20:30 is deliberately given the charging slot 14:30 to 17:30. Normally for a three-hour charging, the user pays 48 Rupees, however EV7 only pays 30 Rupees. This is because at this slot, EV7 is able to get maximum benefit from solar and wind energy (as shown in Fig. 12.8) and is sharing the slot with only one other EV i.e. EV8. A comparison of the optimized load, randomly distributed load, and worst case loads are compared in Fig. 12.12. Under the worst case scenario, all EVs are allowed to charge between 12:00 PM and 14:30 PM; under the randomly distributed scenario (as shown in Fig. 12.11), the load curve is somewhat more distributed but peaking is still there because a substantial number of EVs are charging between 12:00 PM and 15:00 PM; under the optimized scenario, load curve is more distributed and peak is flatter due to distribution in EV charging slots.

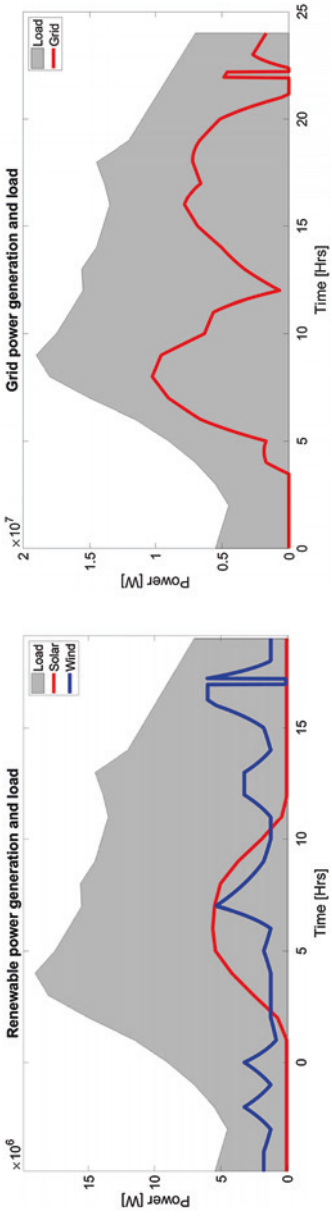


**Fig. 12.7** Load demand, power generated from renewable sources and grid

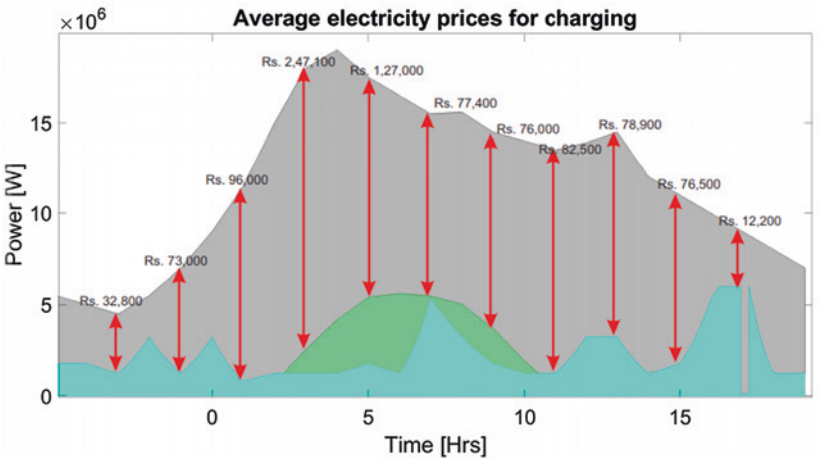


**Fig. 12.8** Average approximate electricity charges in Indian rupees

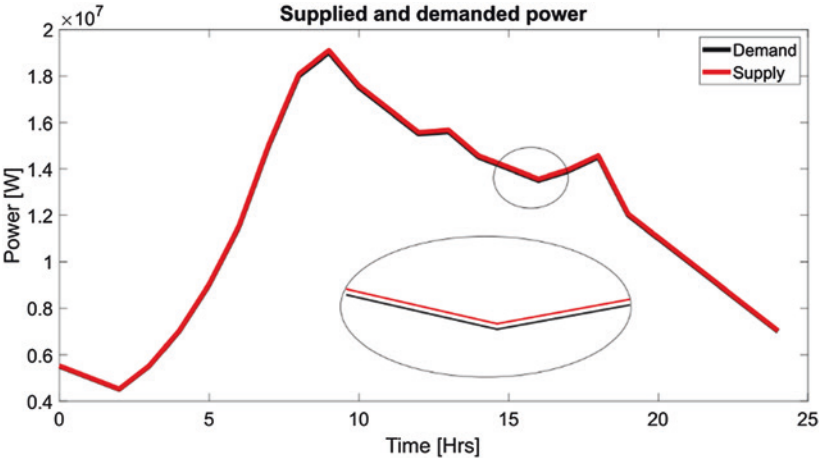


**Fig. 12.9** Power supplied and power demanded

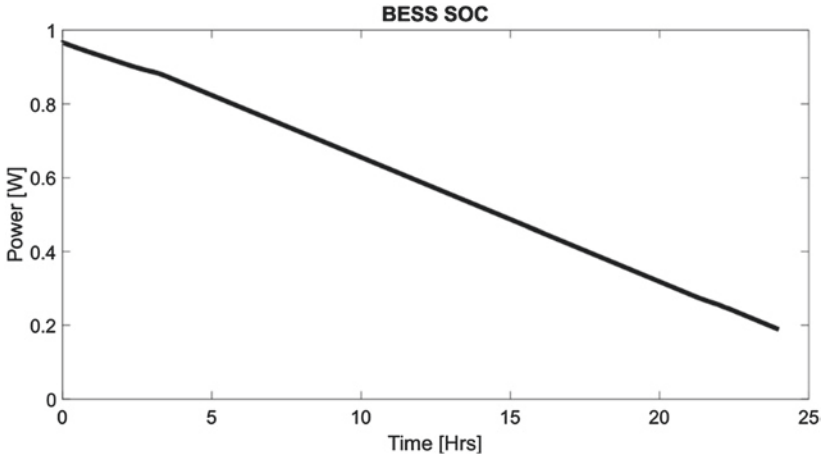


**Fig. 12.10** State of charge of battery energy storage system

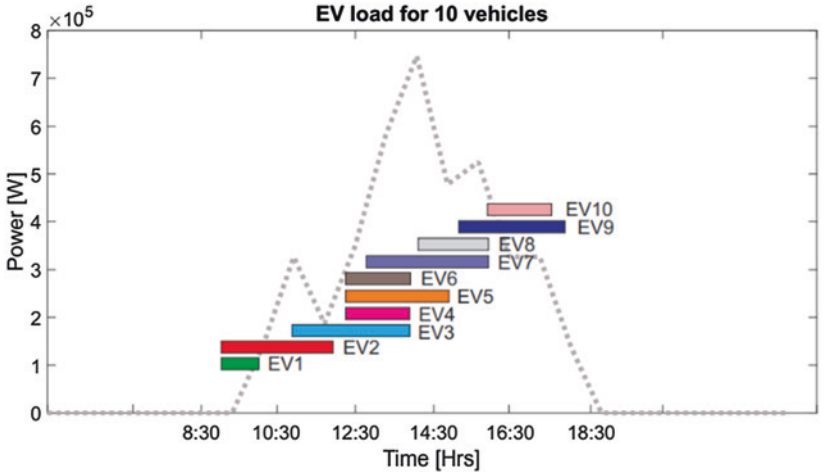


**Fig. 12.11** Load demand with randomly distributed EV charging

**Table 12.4** Case scenario for 10 EVs with randomly distributed charge scheduling

| Number of EV | Charging time slot | Initial SOC | Final SOC | Arrival time | Deadline |
|---|---|---|---|---|---|
| EV1 | 9:30–10:30 AM | 50 | 90 | 7:30 | 10:30 |
| EV2 | 9:00–12:00 PM | 10 | 90 | 8:30 | 17:30 |
| EV3 | 11:00–14:00 PM | 20 | 90 | 10:30 | 17:30 |
| EV4 | 12:00–14:00 PM | 50 | 90 | 10:30 | 17:30 |
| EV5 | 12:00–15:00 PM | 30 | 90 | 10:30 | 17:30 |
| EV6 | 12:00–14:00 PM | 40 | 90 | 11:30 | 17:30 |
| EV7 | 13:00–16:00 PM | 20 | 90 | 11:30 | 20:30 |
| EV8 | 14:00–16:00 PM | 40 | 90 | 11:30 | 20:30 |
| EV9 | 15:00–18:00 PM | 10 | 90 | 14:30 | 20:30 |
| EV10 | 16:00–19:00 PM | 30 | 90 | 14:30 | 20:30 |

**Table 12.5** Case scenario for 10 EVs with optimally distributed charge scheduling

| Number of EV | Charging time slot | Initial SOC | Final SOC | Charging cost (in Rupees) |
|---|---|---|---|---|
| EV1 | 7:30- 8:30 | 50 | 80 | 10 |
| EV2 | 8:30–10:30 | 10 | 60 | 26 |
| EV3 | 10:30–11:30 | 20 | 50 | 14 |
| EV4 | 11:30–13:30 | 50 | 90 | 28 |
| EV5 | 12:30–14:30 | 30 | 80 | 23 |
| EV6 | 11:30–13:30 | 40 | 90 | 20 |
| EV7 | 14:30–17:30 | 20 | 90 | 30 |
| EV8 | 15:30–17:30 | 40 | 90 | 52 |
| EV9 | 17:30–20:30 | 10 | 90 | 40 |
| EV10 | 17:30–19:30 | 30 | 90 | 29 |

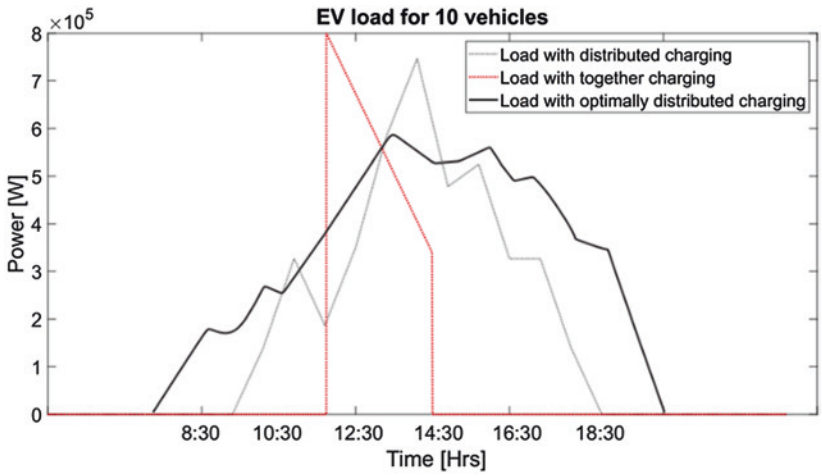


**Fig. 12.12** Load demand with randomly distributed, worst case, and optimally distributed EV charging

## 12.5 Conclusion

In this contribution an optimized charge scheduling of electric vehicles (EVs) is considered as a part of the Energy Management Strategy (EMS) in an integrated renewable-based micro-grid. Here, a solar-wind-battery storage combination is used for renewable energy generation and storage. A conventional grid is also used to compensate for the extra demand hours. One supervisory controller and four local controllers are designed for the task of energy management and control. The main idea is to develop a charge control scheme which checks the initial and final SOCs of each EV and can distribute the charging accordingly. The goal is to develop an optimized charge distribution that define when and how much charging is to be done for each EV. For a certain example scenario where 100 EVs are visiting a university campus or IT park regularly, a central aggregator can be considered managing the charging of 10 EVs at a time. In such a case, three scenarios are developed: a worst case where all EVs are charging together, a random case with distributed charging and a best case with optimally distributed charging. The optimization of charge scheduling with multi-objective genetic algorithm shows that, the two objectives: minimization of electricity cost and maximization of user convenience can be achieved, and the peak load can

be flatted giving the EVs a better benefit in terms of energy cost. In future work, individual driving patterns will be included, optimization of initial SOC and final SOC in more diverse charging scenarios will be in focus.

## Literatur

Alsumiri, M. (2019). Residual incremental conductance based nonparametric MPPT control for solar photovoltaic energy conversion system. *IEEE Access, 7,* 87901–87906. https://doi.org/10.1109/ACCESS.2019.2925687.

Bhatti, A. R., Salam, Z., Aziz, M. J. B. A., Yee, K. P., & Ashique, R. H. (2016). Electric vehicles charging using photovoltaic: Status and technological review. *Renewable and Sustainable Energy Reviews, 54,* 34–47. https://doi.org/10.1016/j.rser.2015.09.091

Bose, B., Kumar Tayal, V., & Moulik, B. (2020). Multi-loop multi-objective control of solar hybrid ev charging infrastructure for workplace. *2020 2nd International Conference on Advances in Computing, Communication Control and Networking (ICACCCN),* 491–496. https://doi.org/10.1109/ICACCCN51052.2020.9362768.

Cao, J., Crozier, C., McCulloch, M., & Fan, Z. (2019). Optimal design and operation of a low carbon community based multi-energy systems considering EV integration. *IEEE Transactions on Sustainable Energy, 10*(3), 1217–1226. https://doi.org/10.1109/TSTE.2018.2864123.

Chandra Mouli, G. R., Bauer, P., & Zeman, M. (2016). System design for a solar powered electric vehicle charging station for workplaces. *Applied Energy, 168*(2016), 434–443. https://doi.org/10.1016/j.apenergy.2016.01.110.

Chandra Mouli, G. R., Kefayati, M., Baldick, R., & Bauer, P. (2019). Integrated PV charging of EV fleet based on energy prices, V2G, and offer of reserves. *IEEE Transactions on Smart Grid, 10*(2), 1313–1325. https://doi.org/10.1109/TSG.2017.2763683.

Chaudhari, K., Ukil, A., Kumar, K. N., Manandhar, U., & Kollimalla, S. K. (2018). Hybrid optimization for economic deployment of ESS in PV-integrated ev charging stations. *IEEE Transactions on Industrial Informatics, 14*(1), 106–116. https://doi.org/10.1109/TII.2017.2713481.

Chung, H. M., Li, W. T., Yuen, C., Wen, C. K., & Crespi, N. (2018). Electric vehicle charge scheduling mechanism to maximize cost efficiency and user convenience. *ArXiv, 10*(3), 3020–3030.

Eldeeb, H. H., Hariri, A. O., Lashway, C. R., & Mohammed, O. A. (2017). Optimal sizing of inverters and energy storage for power oscillation limiting in grid connected large scale electric vehicle park with renewable energy. *2017 IEEE Transportation Electrification Conference and Expo (ITEC), V,* 288–293. https://doi.org/10.1109/ITEC.2017.7993286.

Eldeeb, H. H., Faddel, S., & Mohammed, O. A. (2018). Multi-objective optimization technique for the operation of grid tied PV powered EV charging station. *Electric Power Systems Research, 164,* 201–211. https://doi.org/10.1016/j.epsr.2018.08.004.

Koohi-Kamali, S., Rahim, N. A., & Mokhlis, H. (2014). Smart power management algorithm in microgrid consisting of photovoltaic, diesel, and battery storage plants

considering variations in sunlight, temperature, and load. *Energy Conversion and Management, 84,* 562–582. https://doi.org/10.1016/j.enconman.2014.04.072.

Liu, Y., Li, Y., Liang, H., He, J., & Cui, H. (2019). Energy routing control strategy for integrated microgrids including photovoltaic. Battery-energy storage and electric vehicles. *Energies, 12*(2), 302. https://doi.org/10.3390/en12020302.

M., A., I., A., & M., H. (2013). Maximum power extraction from utility-interfaced wind turbines. In *New developments in renewable energy*. InTech. https://doi.org/10.5772/54675.

M. Ali, A., Moulik, B., & Söffker, D. (2020). Optimizing the fuel efficiency of fuel cell-based hybrid electric vehicles considering real implications. In *Neue Dimensionen der Mobilität* (S. 185–194). Springer Fachmedien. https://doi.org/10.1007/978-3-658-29746-6_17.

Marzband, M., Sumper, A., Domínguez-García, J. L., & Gumara-Ferret, R. (2013). Experimental validation of a real time energy management system for microgrids in islanded mode using a local day-ahead electricity market and MINLP. *Energy Conversion and Management, 76,* 314–322. https://doi.org/10.1016/j.enconman.2013.07.053.

Milis, K., & Peremans, H. (2015). Economical optimization of microgrids: A non-causal model. *Volume 2: Photovoltaics; Renewable-Non-Renewable Hybrid Power System; Smart Grid, Micro-Grid Concepts; Energy Storage; Solar Chemistry; Solar Heating and Cooling; Sustainable Cities and Communities, Transportation; Symposium on Integrated/Sustainable Buil, 2*. https://doi.org/10.1115/ES2015-49634.

Mokrani, Z., Rekioua, D., & Rekioua, T. (2014). Modeling, control and power management of hybrid photovoltaic fuel cells with battery bank supplying electric vehicle. *International Journal of Hydrogen Energy, 39*(27), 15178–15187. https://doi.org/10.1016/j.ijhydene.2014.03.215.

Mukherjee, J. C., & Gupta, A. (2015). A review of charge scheduling of electric vehicles in smart grid. *IEEE Systems Journal, 9*(4), 1541–1553. https://doi.org/10.1109/JSYST.2014.2356559.

Patterson, M., Macia, N. F., & Kannan, A. M. (2015). Hybrid microgrid model based on solar photovoltaic battery fuel cell system for intermittent load applications. *IEEE Transactions on Energy Conversion, 30*(1), 359–366. https://doi.org/10.1109/TEC.2014.2352554.

Robalino, D. M., Kumar, G., Uzoechi, L. O., Chukwu, U. C., & Mahajan, S. M. (2009). Design of a docking station for solar charged electric and fuel cell vehicles. *2009 International Conference on Clean Electrical Power, 2,* 655–660. https://doi.org/10.1109/ICCEP.2009.5211977.

Robledo, C. B., Oldenbroek, V., Abbruzzese, F., & van Wijk, A. J. M. (2018). Integrating a hydrogen fuel cell electric vehicle with vehicle-to-grid technology, photovoltaic power and a residential building. *Applied Energy, 215,* 615–629. https://doi.org/10.1016/j.apenergy.2018.02.038.

Ru, Y., Kleissl, J., & Martinez, S. (2013). Storage size determination for grid-connected photovoltaic systems. *IEEE Transactions on Sustainable Energy, 4*(1), 68–81. https://doi.org/10.1109/TSTE.2012.2199339.

Shi, W., Li, N., Chu, C.-C., & Gadh, R. (2017). Real-time energy management in microgrids. *IEEE Transactions on Smart Grid, 8*(1), 228–238. https://doi.org/10.1109/TSG.2015.2462294.

Stluka, P., Godbole, D., & Samad, T. (2011). Energy management for buildings and microgrids. *IEEE Conference on Decision and Control and European Control Conference, 5150–5157*. https://doi.org/10.1109/CDC.2011.6161051.

Wu, X., Hu, X., Moura, S., Yin, X., & Pickert, V. (2016). Stochastic control of smart home energy management with plug-in electric vehicle battery energy storage and photovoltaic array. *Journal of Power Sources, 333,* 203–212. https://doi.org/10.1016/j.jpowsour.2016.09.157.

Zhang, L., Peng, H., Ning, Z., Mu, Z., & Sun, C. (2017). Comparative research on RC equivalent circuit models for lithium-ion batteries of electric vehicles. *Applied Sciences, 7*(10), 1002. https://doi.org/10.3390/app7101002.

Zhong, Q., Buckley, S., Vassallo, A., & Sun, Y. (2018). Energy cost minimization through optimization of EV, home and workplace battery storage. *Science China Technological Sciences, 61*(5), 761–773. https://doi.org/10.1007/s11431-017-9188-y.